Crustal structure beneath Montserrat, Lesser Antilles, constrained by xenoliths, seismic velocity structure and petrology

Kiddle, E.J.[1], B. Edwards[2], S.C. Loughlin[3], M. Petterson[4], R.S.J. Sparks[1], B. Voight[5].

1. Department of Earth Sciences, University of Bristol, Wills Memorial Building, Queen's Road, Bristol, BS8 1RJ, UK.
2. Department of Geology, Dickinson College, Carlisle, PA 17013-2896, USA.
3. British Geological Survey, Murchison House, West Mains Road, Edinburgh, EH9 3LA, UK.
4. Department of Geology, University of Leicester, Leicester LE1 7RH4, UK.
5. Department of Geosciences, Pennsylvania State University, PA 16802.

Abstract

Noritic anorthosite, gabbroic anorthosite and hornblende-gabbro xenoliths are ubiquitous in the host andesite at Montserrat. Other xenoliths include quartz diorite, metamorphosed biotite-gabbro, plagioclase-hornblendite and plagioclase-clinopyroxenite. Mineral compositions suggest a majority of the xenoliths are cognate. Cumulate, hypabyssal and crescumulate textures are present. A majority of the xenoliths are estimated to have seismic velocities of 6.7-7.0 km/s for vesicle-free assemblages. These estimates are used in conjunction with petrological models to help constrain the SEA CALIPSO seismic data and the structure of the crust beneath Montserrat. Andesitic upper crust is interpreted to overlie a lower crust dominated by amphibole and plagioclase. Xenolith textures and seismic data indicate the presence of hypabyssal intrusions in the shallow crust. The structure of the crust is consistent with petrological models indicating that fractionation is the dominant process producing andesite at Montserrat.

Introduction

The composition of arc crust is a fundamental issue in earth sciences. Seismic surveys suggest that arcs are significantly thicker than oceanic crust, with inferred compositions more mafic than continental crust (e.g. Christensen and Mooney, 1995). Most of our knowledge derives from seismic surveys, exhumed crustal sections and crustal xenoliths. Here igneous xenoliths sampled from andesite lavas on Montserrat are described and used, together with petrological information, to help interpret seismic velocity data obtained from the SEA CALIPSO project. Together these data constrain the crustal structure beneath Montserrat.

Background

Montserrat is located in the Lesser Antilles island arc related to subduction of the Atlantic plate beneath the Caribbean plate. Arc volcanism has been active since the Cretaceous and shifted westward during the Miocene, producing a double island chain. Early seismic surveys determined an average crustal thickness in the Lesser Antilles of ~30km, with a heterogeneous upper crust (V_p=6.2km/s) of variable thickness, and a higher velocity lower crust (V_p=6.9km/s, Westbrook and McCann, 1986; and references therein). However Christeson et al. (2008) reported an average crustal thickness of 24km.

The four volcanic centres of Montserrat date back to 2.6Ma (Harford et al., 2002). The current eruption of Soufrière Hills Volcano (SHV) began in 1995, characterised by phases of dome growth and collapse. Deposits include andesitic domes and pyroclastic, lahar and debris avalanche deposits. Andesite is the dominant rock type. Evidence from deformation studies (Mattioli et al., 1998) and melt inclusions (Devine et al., 1998) indicate a magma chamber at 5-6km depth beneath the SHV. A deeper chamber (~12km) has been inferred from deformation modelling combined with magma extrusion volumes (Elsworth et al., 2008). Mafic magmatic inclusions in the host andesite suggest repeated input of basalt and basaltic andesite magma accompanied by reheating (e.g. Sparks et al., 1998; Murphy et al., 1998).

Methodology

Crustal xenoliths were collected from all four volcanic centres. Modal mineral proportions were obtained for a representative selection of xenoliths, host andesite and mafic magmatic inclusions by point counting using a petrographic microscope. Mineral phases were analysed for major elements using the Cameca SX100 electron microprobe at Bristol University with a 20kV accelerating voltage and 10nA beam current. Textures were analysed using a petrological microscope and the Scanning Electron Microscope (SEM).

The seismic velocity of a rock can be estimated from modal proportions and elastic properties of individual minerals, assuming isotropic fabrics, using the following equation:

$$M^* = \left(\sum_{i=1}^{n} (v_i M_i)^t \right)^{\frac{1}{t}}$$

where M^* is the bulk or shear modulus of the composite; v_i is the volumetric proportion of the *i*th mineral; and M_i is the bulk or shear modulus of the *i*th mineral. The Voigt average (M_V) assumes uniform strain (t=1) and the Ruess average (M_R) assumes uniform stress (t=-1) throughout the polymineralic rock (Watt et al., 1976, and references therein). These averaging schemes effectively provide upper and lower bounds, therefore the arithmetic mean $(M_V+M_R)/2$, or the 'Hill average', is commonly used (Watt et al., 1976). Unless stated otherwise, quoted velocities have been calculated using the arithmetic mean. Elastic constants were taken from the compilation of Hacker and Abers (2004; and references therein). Average mineral compositions from electron probe analyses were used to extrapolate between end-member elastic constants, except for plagioclase (Angel et al., 2004). The effect of porosity on seismic velocities can be estimated using the equation below (Wyllie et al., 1958):

$$\frac{1}{V} = \frac{\phi}{V_f} + \frac{1-\phi}{V_m}$$

where ϕ is fractional porosity, V_f and V_m are the seismic velocities of the pore fluid and the rock matrix respectively.

Bulk rock temperature and pressure corrections of -0.0005 km/s °C^{-1} (Christensen, 1979) and 0.006 s (Rudnick and Fountain, 1995) respectively were used. Velocities were modelled based on a normal arc geothermal gradient of 30 °C/km. Calculated velocity gradients of most rock types compare well to estimates based on temperature and pressure derivatives of individual mineral elastic constants (Hacker and Abers, 2004), with a maximum discrepancy of 0.09 km/s at 20km depth.

Results and Discussion

Xenoliths

Most xenoliths are intrusive igneous rocks. They can be classified as: noritic anorthosites, gabbroic anorthosites, and hornblende-gabbros. Other less common xenoliths include: quartz diorite, metamorphosed biotite-gabbro, and nearly pure (80-86%) monomineralic rocks including: plagioclase-hornblendite and plagioclase-clinopyroxenite. Xenolith modal mineralogy is characterised by varying proportions of plagioclase, amphibole, orthopyroxene, clinopyroxene, titanomagnetite, ilmenite and quartz, similar to mineral assemblages in the host andesite (Table 1). Montserrat xenoliths have similar mineral assemblages to xenoliths found throughout the Lesser Antilles (Arculus and Wills, 1980), apart from the absence of olivine.

The xenoliths are mostly unlayered and isotropic. Sharp contacts with the host andesite and absence of chilled margins suggest the xenoliths were largely or entirely consolidated prior to entrainment, in contrast to the mafic magmatic inclusions (Figure 1). Many of the xenoliths have orthocumulate textures with vesiculated groundmasses (<26vol%) and abundant plagioclase microlites, similar to xenoliths from other Antilles islands (Arculus and Wills, 1980). This indicates the presence of partially quench crystallized interstitial melt (<42%). Miarolitic cavities partially infilled with secondary cristobalite together with the fine-medium grain size indicate that most xenoliths crystallised in hypabyssal intrusions. Some samples display adcumulate and crescumulate textures. One sample consists of alternating pyroxene-anorthosite and plagioclase-clinopyroxenite layers, with crescumulate textures normal to the mineral layering. Such textures are interpreted as rapid crystal growth from a supercooled melt at the margins of a magma body (e.g. Donaldson, 1977).

Plagioclase compositions of most xenoliths (An_{46-91}) show similar variation to the host andesite and mafic inclusions (Murphy et al., 1998). Crystals display normal, reverse and oscillatory zoning consistent with repeated injections of mafic magma, as interpreted for the host andesite (e.g. Sparks et al., 1998; Murphy et al., 1998). Sodic plagioclase microlites (An_{20-37}) are consistent with crystallisation from a late-stage melt.

Mafic phases include clinopyroxene ($En_{37-40}Wo_{38-45}$) ±orthopyroxene ($En_{54-60}Wo_{2-4}$) ±magnesio-hornblende (Leake et al., 1997). No significant core-rim variations are observed in a majority of the xenoliths. Hornblende typically contains 6.3-8.8wt% Al_2O_3, with magnesium numbers of 58-64, a similar range to the host andesite (Murphy et al., 1998). A few xenoliths have more Al-rich hornblende similar to the mafic inclusions (<14wt% Al_2O_3; Murphy et al., 1998). Similar mineral compositions of most xenoliths to the host andesite suggest they are cognate (or there is a primary magmatic relationship). The lack of suitable mineral assemblages has hindered estimates of xenolith equilibration pressures.

Hornblende from plagioclase-hornblendite has significantly higher magnesium numbers of 70-76. The layered sample is compositionally distinct, with highly calcic plagioclase (An_{79-87}) and a small proportion of more magnesium-rich orthopyroxene (En_{65-67}). Sodic plagioclase rims (An_{36-64}) and Fe-rich orthopyroxene rims (En_{46-52}) are present in the pyroxene-anorthosite layer. This sample is interpreted as crystallization at the margins of a mafic magma body, with rim compositions indicative of infiltration of the crystal mush by more evolved melts.

Velocity estimates

Velocity estimates of the xenoliths are very similar despite the range of mineral assemblages (Figure 2). Velocity of most xenoliths calculated from their primary modal mineralogy show good correlation with laboratory measurements of similar rocks (Table 1; Christensen and Mooney, 1995). However calculated velocities of the andesite and mafic magmatic inclusions are significantly higher. Alteration minerals and a small proportion of glass observed in these rocks may produce some of this variation.

Velocities have been calculated based on three scenarios: (1) no vesicles, assuming that vesicles are only abundant in the shallow crust; (2) all vesicles are filled with water; and (3) all vesicles are filled with secondary quartz, based on observed cristobalite (Figure 2). Water-saturated vesicles dramatically reduce seismic velocity estimates by up to 2.9 km/s for the highly vesicular samples. Secondary quartz reduces velocities by <0.3 km/s.

SEA CALIPSO results

The upper crust beneath Montserrat is considered to consist largely of andesite based on surface geology and our new observations of xenoliths formed in shallow intrusions. An intrusive complex could explain the high velocity core beneath the island imaged by the SEA CALIPSO project (Paulatto et al., in press; Shalev et al., this issue). The calculated seismic velocity of andesite is much higher pore-free than observed velocities, indicating that porosity is an important control of velocity in the uppermost crust (0-5km). Field observations indicate that volcaniclastic rocks likely dominate the near–surface, with primary and secondary porosity from vesicles and inter-particle spaces. At the greatest resolvable depth (~8km; Paulatto et al., in press) seismic tomography results are lower than all calculated pore-free velocities.

Sevilla et al. (subjudice) have produced a receiver function profile that resolves the Moho at ~30km depth. A mid-crustal layer ~1km thick with velocities of 6.0-6.7 km/s is consistent with measured (Christensen and Mooney, 1995) and calculated velocities of quartz diorite. Lower crustal velocities of 6.7-7.0 km/s (Sevilla et al., subjudice) match estimated velocities of plagioclase-hornblendite and basaltic to basaltic andesite mafic inclusions, and measured velocities of gabbro, norite, anorthosite and hornblendite (Figure 3; Christensen and Mooney, 1995). Relict oceanic crust may also be present in the lower crust.

Constraints from petrology

Several igneous processes can lead to layering of island arc crust, including partial melting of older crust and crystallisation of basalt, together with segregation of residual evolved melts. These scenarios produce physically similar layering with more differentiated magma supplied to the upper crust leaving denser more mafic cumulates or restite in the lower crust (Annen et al., 2006). Thus it is difficult to distinguish between these processes from seismic velocity data alone.

Magmatic parents to the andesite magma could be represented by the mafic inclusions or the South Soufrière Hills basaltic andesite. Zellmer et al. (2003) calculated that the most evolved mafic inclusion could be produced from the least evolved mafic inclusion by fractional crystallisation of 49% amphibole and 21% plagioclase. A further ~10% crystallisation is necessary to produce the Th concentration of the most evolved andesite. The andesite can also be modelled by 65% crystallisation of plagioclase and amphibole from the least evolved South Soufrière Hills lava (Zellmer et al., 2003).

Fractionation models (Zellmer et al., 2003) thus imply that an andesitic upper crust should be complemented by cumulates of plagioclase and amphibole in the lower crust. Upper/middle crust interpreted from the receiver function profile (Sevilla et al., subjudice) is ~10km thick to the island surface, and lower crust is ~21km thick. The ratio of upper to lower crust is therefore 1:2. This is consistent with the 65% South Soufrière Hills fractionation model (Zellmer et al., 2003). Without a 3D velocity structure we cannot account for the lateral extent of crustal layers. Assuming the lower crust dominantly comprises plagioclase and amphibole, observed seismic velocities (Sevilla et al., subjudice) correspond to 30-80% hornblende and corresponding plagioclase. These fractionation models are based on a parental magma that is evolved with respect to primitive melts. Therefore additional cumulates of pyroxene, olivine and plagioclase are either present in the lower crust or beneath the petrological Moho, noting that the velocities of these ultramafic cumulates could be >7.7 km/s.

Some evidence indicates that the andesite is at least partially produced by anatexis. Stable isotope ratios of amphiboles (Harford and Sparks, 2001) and bulk U/Th ratios indicate partial melting and remobilisation of previous intrusions (Zellmer et al., 2003). Tatsumi et al. (2008) suggest that ~30% melting of basaltic crust could produce andesitic magma. This would produce a middle to lower crust ratio of 1:2 also similar to the observed crustal structure. Oxygen isotopes are consistent with a contribution of 10-20% hydrothermally altered crust. However trace element concentrations can largely be modelled by fractional crystallisation (Zellmer et al., 2003). The presence of cumulate textured xenoliths, together with petrological and geochemical evidence, favours a dominant role of intrusion and fractionation of incremental additions of basalt in the model of arc crust formation at Montserrat.

Conclusion

Igneous xenoliths are present in the host lavas at Montserrat, with cumulate and hypabyssal textures. Most have mineral assemblages and mineral compositions indicating that they represent hypabyssal intrusive equivalents of the andesite, or cumulate rocks formed by fractionation of basaltic andesite and andesite. The presence of partially infilled vesicles in most xenoliths indicates shallow crystallisation. Surface geology and seismic velocities (Paulatto et al., in press) are most consistent with an upper crust composed of andesitic volcanic and related intrusive rocks. The xenoliths and fast velocity regions beneath the volcanic centres of Montserrat (Paulatto et al., in press; Shalev et al., this issue) support the interpretation of intrusive complexes. Petrological models (Zellmer et al., 2003) suggest the lower crust contains cumulate rocks dominated by amphibole and plagioclase, which is consistent with seismic velocities (Sevilla et al., subjudice). The proportion of upper intermediate crust to cumulate or restitic lower crust indicates that andesite has been produced by fractionation of the South Soufrière Hills lava (Zellmer et al., 2003) or partial melting of an initial basaltic crust (Tatsumi et al., 2008). A model of arc crust formation largely by fractionation is consistent with xenoliths, petrology and the SEA CALIPSO seismic velocity data.

Acknowledgements

This work is funded by the Natural Environment Research Council and the British Geological Survey. EJK acknowledges Natalie Starkey, Amy Dabrowa and the Montserrat Volcano Observatory for help in the field. EJK also thanks Stuart Kearns for help with EMPA analyses and Richard Arculus for useful discussion. RSJS acknowledges support of a European Research Council Advanced grant.

References

Angel, R. (2004), Equations of state of plagioclase feldspars, *Contrib. Mineral. Petrol.*, *146*(4), doi: 10.1007/s00410-003-0515-5.

Annen, C., J.D. Blundy and R.S.J. Sparks (2006), The Genesis of Intermediate and Silicic Magmas in Deep Crustal Hot Zones, *J. Petrol.*, *47*(3): 505-539.

Arculus, R. and K. Wills (1980), The petrology of plutonic blocks and inclusions from the Lesser Antilles island arc, *J. Petrol.*, *21*(4), 743-799.

Christensen, N.I. and W.D. Mooney (1995), Seismic velocity structure and composition of the continental crust: A global view, *J. Geophys. Res.*, *100*(B6), 9761-9788.

Christensen, N.I. (1979), Compressional wave velocities in rocks at high temperatures and pressures, critical thermal-gradients, and crustal low-velocity zones, *J. Geophys. Res.*, *84*(B12), 6849-6857.

Christeson, G.L., P. Mann, A. Escalona, T.J. Aitken (2008), Crustal structure of the Caribbean-northeastern South America arc-continent collision zone, *J. Geophys. Res.*, *113*(B8), B08104, doi: 10.1029/2007JB005373.

Devine, J.D., M.D. Murphy, M.J. Rutherford, J. Barclay, R.S.J. Sparks, M.R. Carroll, S.R. Young, J.E. Gardner (1998), Petrologic evidence for pre-eruptive pressure-temperature conditions, and recent reheating, of andesitic magma erupting at the Soufriere Hills Volcano, Montserrat, WI, *Geophys. Res. Lett.*, *25*(19), 3669-3672.

Donaldsson, C.H. (1977), Laboratory duplication of comb layering in the Rhum pluton, *Min. Mag.*, 41, 323-336.

Elsworth, D., G. Mattioli, J. Taron, B. Voight (2008), Implications of Magma Transfer Between Multiple Reservoirs on Eruption Cycling, *Science*, *322*(5899), 246-248, doi: 10.1126/science.1161297.

Shalev, E. et al. (this volume), 3-D Seismic Velocity Tomography of Montserrat From the SEA-CALIPSO Offshore/Onshore Experiment. *Geophys. Res. Lett.*, Special Section on Montserrat.

Hacker, B. and G. Abers (2004), Subduction Factory 3: An Excel worksheet and macro for calculating the densities, seismic wave speeds, and H2O contents of minerals and rocks at pressure and temperature, *Geochem. Geophys. Geosyst.*, *5*, Q01005, doi: 10.1029/2003GC000614.

Harford, C.L. and R.S.J. Sparks (2001), Recent remobilisation of shallow-level intrusions on Montserrat revealed by hydrogen isotope compositions of amphiboles, *Earth Planet. Sci. Lett.*, *185*(3-4), 285-297.

Harford, C.L., M.S. Pringle, R.S.J. Sparks, S.R. Young (2002), The volcanic evolution of Montserrat using ^{40}Ar/^{39}Ar geochronology, in *The eruption of the Soufriere Hills Volcano, Montserrat, from 1995 to 1999*, edited by Druitt, T. H. and B.P. Kokelaar (eds), Geological Society, London, Memoir 21, pp. 93-113.

Leake, B.E., et al. (1997), Nomenclature of amphiboles: report of the subcommittee on amphiboles of the international mineralogical association, commission on new minerals and mineral names, *The Can. Mineral.*, *35*, 219-246.

Mattioli, G. S., T. H. Dixon, F. Farina, E. S. Howell, P. E. Jansma, A. L. Smith (1998), GPS measurement of surface deformation around Soufriere Hills volcano, Montserrat from October 1995 to July 1996, *Geophys. Res. Lett.*, *25*(18), 3417-3420.

Murphy, M., S. Loughlin, J. Devine, S. Sparks (1998), The role of magma mixing in triggering the current eruption at the Soufriere Hills volcano, Montserrat, West Indies, *Geophys. Res. Lett.*, *25*(18), 3433-3436.

Paulatto, M., et al. (2009), Upper crustal structure of an active volcano from refraction/reflection tomography, Montserrat, Lesser Antilles, *Geophys. J. Int.*, in press.

Rudnick, R.L. and D.M. Fountain (1995), Nature and composition of the continental crust: a lower crustal perspective, *Rev. Geophys.*, *33*, 267-309.

Sevilla, W., C. J. Ammon, and B. Voight (subjudice), Crustal Structure Beneath the Montserrrat Region of the Lesser Antilles Island Arc, *Geophys., Geochem., Geosyst.*

Sparks, R.S.J., S. Young, J. Barclay, E. Calder (1998), Magma production and growth of the lava dome of the Soufrière Hills Volcano, West Indies: November 1995 to December 1997, *Geophys. Res. Lett.*, *25*(18), 3421-3424.

Tatsumi, Y., H. Shukuno, K. Tani, N. Takahashi, S. Kodaira, T. Kogiso (2008), Strusture and growth of the Izu-Bonin-Mariana arc crust: 2. Role of crust-mantle transformation and the transparent Moho in arc crust evolution, *J. Geophys. Res.*, *113*, B02203, doi: 10.1029/2007JB005121.

Watt, J.P., G.F. Davies, and R.J. O'Connell (1976), The elastic properties of composite materials, *Rev. Geophys.*, *14*(4), 541-563.

Westbrook, G.K. and W.R. McCann (1986), Subduction of Atlantic lithosphere beneath the Caribbean, in *The Geology of North America*, edited by Vogt, P.R. and Tucholke, B.E., The Western North Atlantic Region, vol. M, The Geological Society of America, p.341–350.

Wyllie, M., A. Gregory and G. Gardner (1958), An experimental investigation of factors affecting elastic wave velocities in porous media, *Geophysics*, *23*(3), 459-493.

Zellmer, G.F., C.J. Hawkesworth, R.S.J. Sparks, L.E. Thomas, C.L. Harford, T.S. Brewer, S.C. Loughlin (2003a), Geochemical evolution of the Soufriere Hills volcano, Montserrat, Lesser Antilles volcanic arc, *J. Petrol.*, *44*(8), 1349-1374.

Figure Captions

Figure 1. SEM images of a. diktytaxitic mafic magmatic inclusion, b. hypabyssal-textured noritic anorthosite c. hornblende-gabbro xenolith with adcumulate texture, d. crescumulate clinopyroxene at boundary of pyroxene-anorthosite layer (pl=plagioclase, hb=hornblende, px=pyroxene, mg=titanomagnetite, black=vesicles).

Figure 2. The effect of porosity on estimated compressional wave velocities. Average velocities of each rock type are plotted with error bars corresponding to the range of vesicle contents.

Figure 3. Compressional wave velocities derived from a. estimates based on mineral proportions, and b. laboratory measurements of similar rocks (Christensen and Mooney, 1995; see Table 1 for details). Seismic velocity profiles obtained from the SEA CALIPSO project are also shown (Paulatto et al., in press; Sevilla et al., subjudice).

Table 1: Vesicle-free mineral proportions, calculated compressional wave velocities and laboratory velocity measurements of the main rock types.

Rock type	Mineral proportions (%)						Velocity estimates (km/s)			Velocity Measurements[a] (km/s)
	plg	hb	opx	cpx	ox.	qtz	Voigt	Ruess	Hill	
Hb-gabbro	58-72	21-38	0-6	0-1	2-4	0	6.84-6.96	6.67-6.74	6.75-6.85	7.10±0.25[b]
Noritic and gabbroic anorthosites	70-86	0	2-20	0-13	2-8	0	6.80-7.01	6.63-6.69	6.72-6.83	6.89±0.21[c]
Quartz diorite	69-70	12-15	4-6	0	1-2	7-12	6.69-6.79	6.46-6.54	6.57-6.67	6.44±0.17[d]
Plagioclase-hornblendite	17	83	0	0	0	0	7.08	7.01	7.05	7.11±0.04[e]
Plagioclase-clinopyroxenite	14-16	0	2	79-81	3	0	7.58-7.60	7.43-7.45	7.51-7.52	7.71±0.11[f]
Andesite	73-89	0-5	2-7	1-2	3-8	minor	6.76-6.90	6.58-6.60	6.68-6.74	5.43±0.28
Mafic Inclusion	65	5-28	2-8	2-16	3-6	0	6.98-7.13	6.81-6.83	6.89-6.98	5.88±0.55[g]

[a] Measured at pressure equivalent to 5km depth (Christensen and Mooney, 1995)
[b] Gabbro-norite-troctolite
[c] Anorthosite
[d] Diorite
[e] Hornblendite
[f] Pyroxenite
[g] Basalt

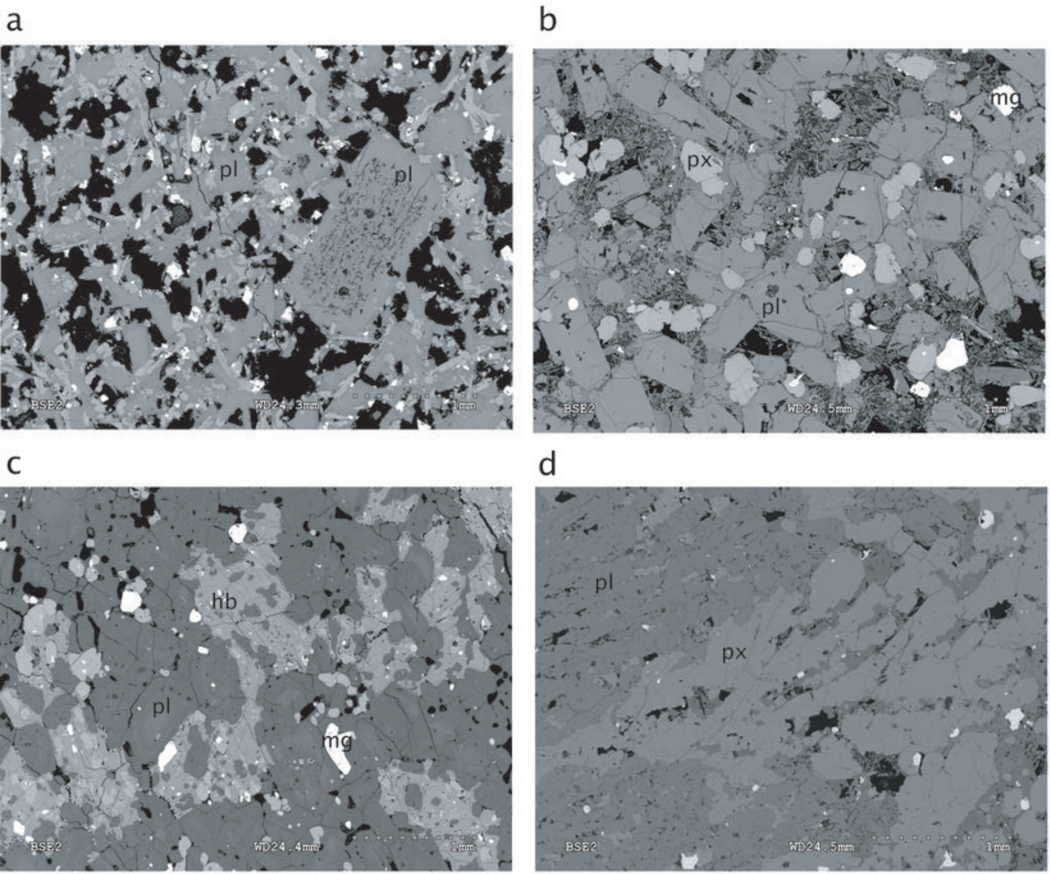

Figure 1. SEM images of a. diktytaxitic mafic magmatic inclusion, b. hypabyssal-textured noritic anorthosite, c. hornblende-gabbro xenolith with adcumulate texture, d. crescumulate clinopyroxene at boundary of pyroxene-anorthosite layer (pl=plagioclase, hb=hornblende, px=pyroxene, mg=titanomagnetite, black=vesicles).

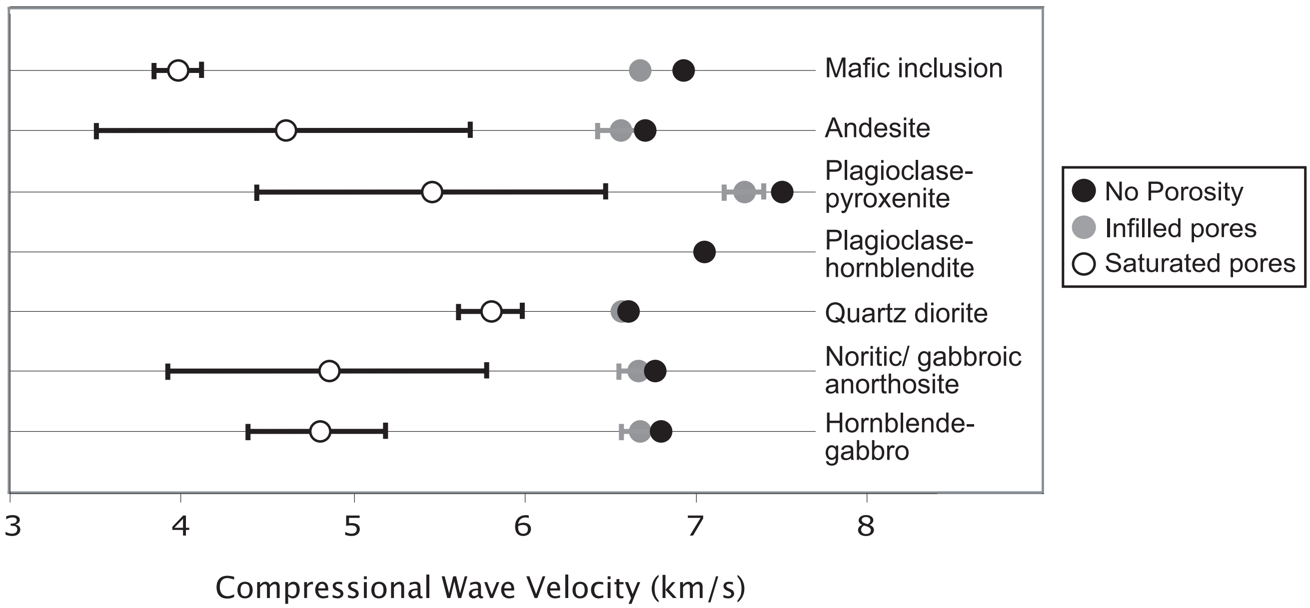

Figure 2. The effect of porosity on estimated compressional wave velocities. Average velocities of each rock type are plotted with error bars corresponding to the range of vesicle contents.

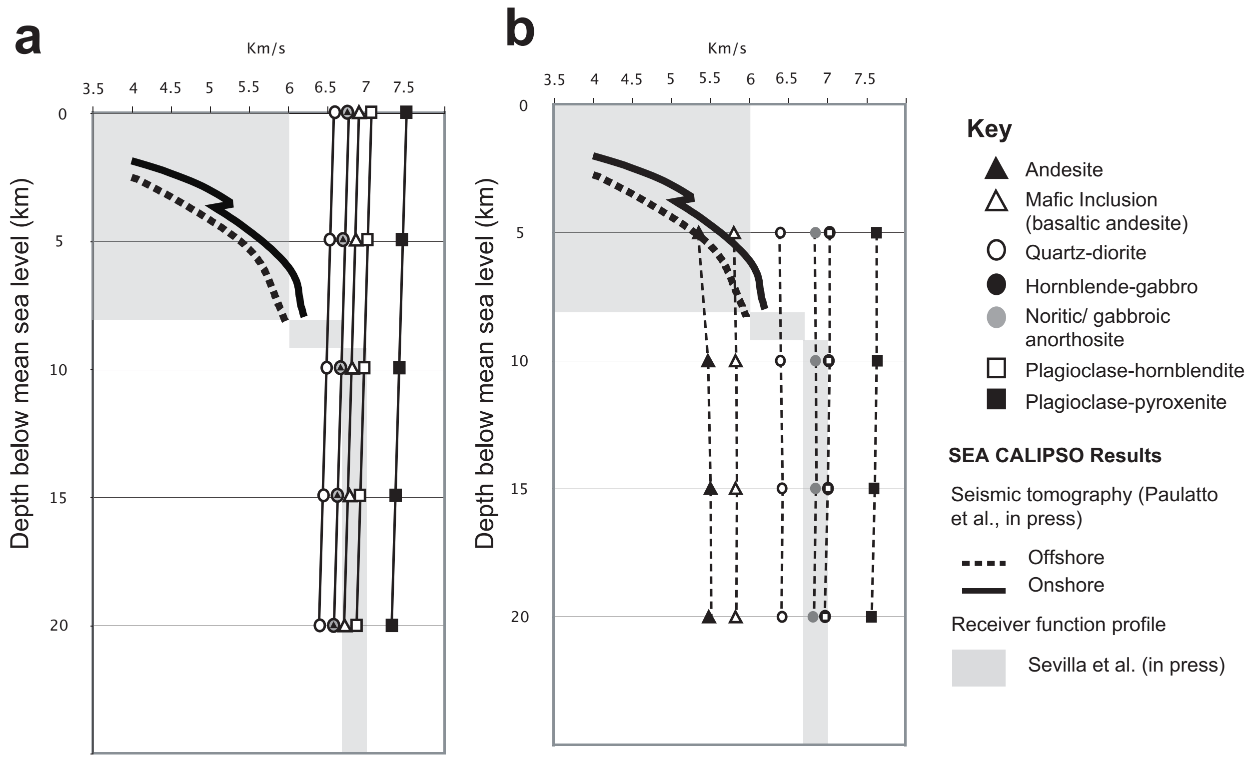

Figure 3. Compressional wave velocities derived from a. estimates based on mineral proportions, and b. laboratory measurements of similar rocks (Christensen and Mooney, 1995; see Table 1 for details). Seismic velocity profiles obtained from the SEA CALIPSO project are also shown (Paulatto et al., in press; Sevilla et al., subjudice).